Phase transitions of H_2 adsorbed on the surface of single carbon nanotubes

M.C. Gordillo[1] and J. Boronat[2]

[1]*Departamento de Sistemas Físicos, Químicos y Naturales, Facultad de Ciencias Experimentales, Universidad Pablo de Olavide, Carretera de Utrera, km 1. 41013 Sevilla, Spain*

[2]*Departament de Física i Enginyeria Nuclear, Universitat Politècnica de Catalunya, Campus Nord B4-B5, 08034 Barcelona, Spain*

(Dated: January 16, 2014)

By means of Diffusion Monte Carlo calculations, we obtained the complete phase diagrams of H_2 adsorbed on the outer surface of isolated armchair carbon nanotubes of radii ranging from 3.42 to 10.85 Å. We only considered density ranges corresponding to the filling of the first adsorption layer in these curved structures. In all cases, the zero-temperature ground state was found to be an incommensurate solid, except in the widest tube, in which the structure with lowest energy is an analogous of the $\sqrt{3}\times\sqrt{3}$ phase found in planar substrates. Those incommensurate solids result form the arrangement of the hydrogen molecules in circumferences whose plane is perpendicular to the main axis of the carbon nanotube. For each tube, there is only one of such phases stable in the density range considered, except in the case of the (5,5) and (6,6) tubes, in which two of these incommensurate solids are separated by novel first order phase transitions.

I. INTRODUCTION

A carbon nanotube is a cylindrical structure[1] that can be thought as the result of the wrapping up of a single graphene sheet[2,3] over itself. In the same way that , in the past , graphene sheets were always found stacked to form graphite, carbon nanotubes were always found forming nanotube bundles, structures in which the only surfaces available for adsorption were the exposed parts of the tubes in the fringes of the bundle[4–6]. The adsorbed phases in a planar structure such as graphite are quite different from the ones observed on a highly patterned substrate like the external surface of a nanotube bundle. This can be seen by comparing the results on a bundle of carbon nanotubes and graphite for ^{4}He[7,8] (bundles)[9,10] (graphite), H_2[14,15] (bundles)[11–13] (graphite), and Ne[16,17] (bundles) and[18,19] (graphite). Similar to the opportunities for adsorption that the achievement of a single graphene sheet offers, a recent experimental work shows the proper technique to suspend a single carbon nanotube and study the phases of different gases (Ar,Kr) adsorbed on its external surface[20]. In this latter work, the results indicated that the phase diagrams were similar to those of the same gases on graphite, but with phase transitions shifted to higher pressures. In the present work, we have studied the adsorption behavior of H_2 on a series of armchair ((n,n)) carbon nanotubes with different diameters in order to see if a quantum gas would exhibit novel phases when adsorbed on curved surfaces. The carbon nanotubes considered, together with their indexes and radii, are given in Table I. The most noticeable results driven from our calculations are: *i*), the existence of a solid-solid phase transition for (5,5) and (6,6) nanotubes, and *ii*), the stability of the curved version of the $\sqrt{3}\times\sqrt{3}$ commensurate phase only for the widest nanotube studied (16,16).

II. METHOD

Our calculations were performed with the diffusion Monte Carlo (DMC) method. This well-established technique allows us to solve exactly the Schroedinger equation within some statistical errors to obtain the ground state energy of a system of interacting bosons[21]. This is exactly our case, since in its lowest energy state (*para*-H_2) the hydrogen molecule behaves as a boson. To apply the DMC algorithm, we need the potentials to describe the H_2-H_2 interaction (we chose the Silvera and Goldman expression[22], a standard model for calculations involving *para*-H_2), and the C-H_2 one. For the latter, we used a Lennard-Jones potential with parameters taken from Ref. 23, as used previously to describe the phase diagram of H_2 adsorbed on graphene[13]. All the individual C-H_2 pairs were considered, i.e., we took into consideration the corrugation effects due to the real structure of the nanotube.

The last ingredient needed to perform a calculation in a DMC scheme is a trial wave function. It regulates the Monte Carlo importance sampling, and can be considered as a variational approximation to the exact description of the system. In this work, we used a trial wave function formed by the product of two terms. The first one is

$$\Phi(\mathbf{r}_1,\mathbf{r}_2,\ldots,\mathbf{r}_N)=\prod_{i<j}\exp\left[-\frac{1}{2}\left(\frac{b_{\mathrm{H_2\text{-}H_2}}}{r_{ij}}\right)^5\right] \qquad (1)$$

$$\times\prod_i\prod_J\exp\left[-\frac{1}{2}\left(\frac{b_{\mathrm{C\text{-}H_2}}}{r_{iJ}}\right)^5\right]\prod_i\exp(-a(r_i-r_0)^2)\ ,$$

where $\mathbf{r}_1$, $\mathbf{r}_2$, ..., $\mathbf{r}_N$ are the coordinates of the H_2 molecules and $\mathbf{r}_J$ the position of the carbon atoms in the nanotube. The first term in Eq. (1) is a two-body Jastrow function depending on the H_2 intermolecular distances r_{ij}, while the second one has the same meaning but for each r_{iJ} (C-H_2). Finally, the third term is a prod-

TABLE I. Armchair carbon nanotubes considered in this work, together with their tube radii (r_t) and the most probable distance for an adsorbed hydrogen molecule to the center of the cylinder (r_0). In the last column, the adsorption energy of a single H_2 molecule (e_0) is reported.

Tube	r_t (Å)	r_0 (Å)	e_0 (K)
(5,5)	3.42	6.36	-320.6 ± 0.1
(6,6)	4.10	7.05	-329.0 ± 0.1
(7,7)	4.75	7.70	-335.5 ± 0.1
(8,8)	5.45	8.39	-341.0 ± 0.1
(10,10)	6.80	9.75	-349.2 ± 0.2
(12,12)	8.14	11.10	-353.7 ± 0.2
(14,14)	9.49	12.46	-356.5 ± 0.1
(16,16)	10.85	13.80	-357.2 ± 0.2

uct of one-body Gaussians with $r_i = \sqrt{x_i^2 + y_i^2}$, that depend on the distance of each H_2 to the center of the tube (r_0).

Equation 1 is appropriate for describing liquid phases, but if the system is a solid, we need to multiply the trial wave function above (1) by

$$\prod_i \exp\left\{-c\left[(x_i - x_{\rm site})^2 + (y_i - y_{\rm site})^2 + (z_i - z_{\rm site})^2\right]\right\} , \quad (2)$$

whose purpose is to limit the location of the hydrogen molecules to regions close to the $x_{\rm site}, y_{\rm site}, z_{\rm site}$ regularly distributed coordinates of a solid arrangement. The variational parameters appearing in the whole trial wave function ($b_{\rm H_2\text{-}H_2}$, $b_{\rm C\text{-}H_2}$, a and c) were fixed to be the same values than the ones for H_2 adsorbed on graphene[13], after having checked that there were no appreciable differences when variationally optimized for the (5,5) tube, i.e. $b_{\rm H_2\text{-}H_2} = 3.195$ Å, $b_{\rm C\text{-}H_2} = 2.3$ Åand $a = 3.06$ Å^{-2}. Parameter c was varied with density in the same way than for graphene. The only remaining parameter, r_0, was optimized independently for each tube; the results are listed in Table I.

III. RESULTS

Table I contains also the binding energies (e_0) of a single H_2 molecule on top of the series of nanotubes considered in this work. We observe, quite reasonably, that this energy increases with the radius of the cylinder. However, even the value for the (16,16) tube is quite far from the result on a flat graphene sheet (-431.79 ± 0.06 K[13]), due to the surface curvature, that distorts the C-H_2 distances with respect to those of a flat graphene sheet.

Our aim in the present work is to describe the possible phases of H_2 adsorbed on the surface of different (n,n) nanotubes. To do so, we considered the curved counterparts of all the commensurate solid phases found experimentally for most of the quantum gases (^{4}He, H_2 and D_2) on graphite[9,11,12,26], which included the curved version of a $\sqrt{3} \times \sqrt{3}$ phase, perfectly possible in these (n,n) tube substrates[20]. For the incommensurate phases,

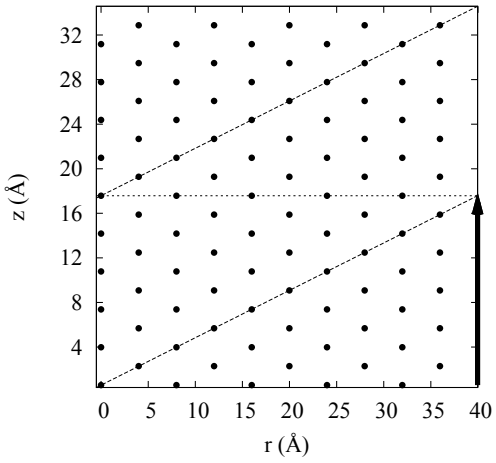

FIG. 1. Projection on a flat surface of an incommensurate structure corresponding to an areal density of 0.076 Å^{-2} to be wrapped around a (5,5) tube. It can be described as an set of five intertwined helices whose pitch (indicated by an arrow) is 17 Å. Every turn of the helix contains 10 H_2 molecules.

we tried structures similar to the triangular phases found in graphene, but wrapped up around to form hydrogen cylinders of radius r_0 (see Table I). One of these structures is shown in Fig. 1, which displays the projections on a plane of the H_2 site locations for an incommensurate solid wrapped around a (5,5) tube. Here, the r coordinate represents the hydrogen positions on a circumference of radius $r_0 = 6.36$ Å, while the z axis is chosen parallel to the main axis of the tube. One can see that the solid is built by locating five H_2 molecules in circumferences on planes perpendicular to z, and rotating the molecules in neighboring circumferences half the distance between H_2 molecules. We defined a phase by the number of hydrogen molecules in one of such circumferences, and varied their density by changing the distance between them. Alternatively, this structure can be thought as the result of having five helices of pitch 17 Åwrapped around the tube, each one of them including 10 molecules per turn of the helix.

DMC results for the equations of state corresponding to different phases of H_2 adsorbed on a (5,5) tube are shown in Fig. 2. Open squares indicate a liquid phase (obtained by considering as a trial function only Eq. (1)), while the circles represent solid incommensurate phases with five (full circles) and six (open circles) H_2 molecules

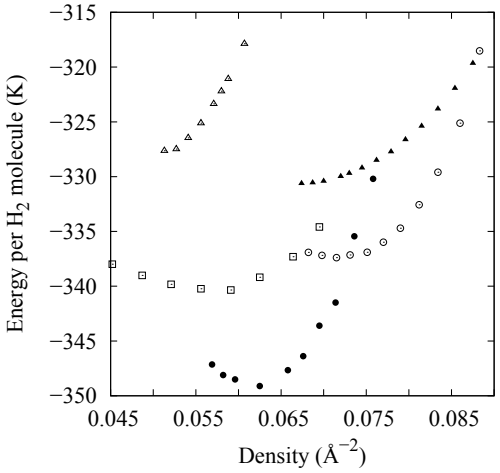

FIG. 2. Energies per H_2 molecule for different adsorbed phases on a (5,5) tube. We display here the liquid (open squares), the different incommensurate solids: five-in-a-row (solid circles), six-in-a row (open circles), four-in-a-row (open triangles) and seven-in-a-row (full triangles).

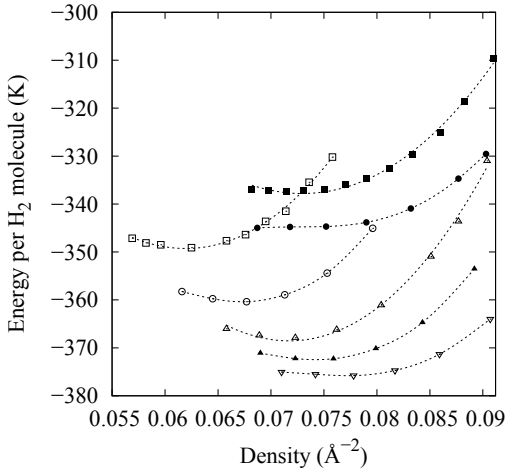

FIG. 3. Equation of state for the incommensurate solids adsorbed in carbon nanotubes of increasing radii: (5,5), (open squares, five-in-a-row solid; full squares, six-in-a-row arrangement); (6,6), (open circles, six-in-a-row structure; full circles, seven-in-a-row solid); (7,7), (open triangles); (8,8), (full triangles); (10,10), (inverted triangles). See further explanation in the text.

per row. We display with triangles results for a four molecules per row (open), and seven molecules per row (full) arrangements. For all the areal densities considered (up to 0.0937 Å^{-2}, the experimental density for a second layer promotion in planar graphite[19]), these last two phases are unstable (of higher energy) with respect to the first two. All the alternative commensurate structures are also unstable, as can be seen in Table II and III. In that table, we also display their areal densities, different for different tubes, even though the pattern of the adsorbed hydrogen molecules is the same. This is due to the fact that the areal densities depend on r_0, while these phases are registered with respect to structures whose dimensions depend on r_t. Other solid incommensurate structures, such as helices with different number of molecules per turn but with the same pitch, i.e., more or less H_2 molecules on top of the dashed lines in Fig. 1, have energies greater than the phases represented by the circles in Fig. 2. For instance, a structure with eleven molecules per turn, instead of the ten displayed in Fig. 1, has a minimum energy of -336.0 ± 0.1 K, for a density of 0.062 ± 0.003 Å^{-2}. Therefore, the ground state of H_2 adsorbed in the outer surface of a (5,5) carbon nanotube is an incommensurate solid with five H_2's per row. Upon a density increase, there is a first-order solid-solid phase transition to another incommensurate solid, similar to the first one but with six atoms per row. The equilibrium densities for both structures at the transition are obtained from a double tangent Maxwell construction: 0.0685 ± 0.0001 Å^{-2} (five molecules per row, energy per hydrogen molecule -345.3 ± 0.1 K) and 0.0795 ± 0.0001 Å^{-2} (six intertwined helices, with energy per hydrogen molecule -334.7 ± 0.1 K).

The stable phases of H_2 on other (n,n) tubes, up to n = 14, are similar to the (5,5) one. In all cases, the ground states are the same type of incommensurate solids already described, the only difference being the number of intertwined helices (or molecules in the same circumference) forming the structure. This number was found to be always equal to the index n of the nanotube. In Fig. 3, we show the equation of state for some of such solids, from the already displayed (5,5) case (open circles; five molecules in a row), to the (10,10) one (inverted open triangles; ten molecules in a row), going through the (6,6) (open circles), (7,7) (open triangles) and (8,8) (full triangles) tubes. In all cases the dashed lines are mere guides-to-the-eye. Between the two narrowest cylinders and the rest there is an important difference, though: the (6,6) tube exhibits a first order phase transition between two incommensurate solids with six and seven molecules per row while, while for the other tubes, there is only one stable incommensurate structure in the areal density range corresponding to an adsorbed monolayer The zero-pressure densities and energies corresponding to the ground state for all the tubes considered are given in Table II. There, and in Table III, we can see that those incommensurate solids are the truly ground states for the systems under consideration at zero pressure, since their energies are lower than the corresponding to any of the commensurate structures on the same tubes. The only exception is the (16,16) nanotube, in which the ground state is the same $\sqrt{3} \times \sqrt{3}$ structure than in a flat sur-

TABLE II. Energies per particle (e_b) and equilibrium densities (ρ) for different phases proposed in the literature[9] for quantum gases on graphite, when adsorbed in tubes of different radii. The liquid and incommensurate helical densities are the values corresponding to the minimum energies obtained by means of third-degree polynomial fits to curves of the type displayed in Fig. 1. The rest correspond to exact densities. Error bars within parenthesis represent the uncertainty of the last figure shown.

Phase	liquid		2/5		3/7		$\sqrt{3}\times\sqrt{3}$		helical incommensurate	
Tube	ρ (Å^{-2})	e_b (K)	ρ (Å^{-2})	e_b (K)	ρ (Å^{-2})	e_b (K)	ρ (Å^{-2})	e_b (K)	ρ (Å^{-2})	e_b (K)
(5,5)	0.0574(4)	-340.3(1)	0.0407	-333.7(2)	0.0436	-325.4(2)	0.0339	-329.03(4)	0.0621(3)	-349.0(2)
(6,6)	0.0586(3)	-349.70(9)	0.0441	-344.4(1)	0.0472	-334.3(2)	0.0367	-339.52(6)	0.0673(1)	-360.34(4)
(7,7)	0.0615(6)	-356.2(2)	0.0471	-352.28(7)	0.0504	-339.7(2)	0.0392	-347.66(3)	0.0716(1)	-367.89(5)
(8,8)	0.0611(7)	-360.3(2)	0.0494	-358.9(1)	0.0529	-343.4(2)	0.0411	-354.44(3)	0.0742(1)	-372.43(3)
(10,10)	0.0578(3)	-365.95(6)	0.0531	-367.11(8)	0.0569	-347.5(2)	0.0443	-364.12(5)	0.0758(1)	-375.6(1)
(12,12)	0.0565(4)	-369.1(1)	0.0559	-371.8(1)	0.0600	-346.3(3)	0.0466	-369.93(5)	0.0703(2)	-375.96(5)
(14,14)	0.0530(4)	-370.4(1)	0.0581	-373.5(1)	0.0623	-342.5(3)	0.0485	-373.10(8)	0.0681(2)	-375.3(1)
(16,16)	0.0511(8)	-367.57(9)	0.0600	-371.17(5)	0.0643	-333.8(3)	0.0500	-371.7(1)	0.0660(1)	-371.4(1)

TABLE III. Same than in Table II, but for two other commensurate structures found experimentally for D_2 on graphite. The dimensions of their unit cells make them only possible for the tubes shown. In all cases, they are unstable with respect to the incommensurate structures (n$\leq$ 14) or to the $\sqrt{3}\times\sqrt{3}$ one (n= 16).

$7/16$[25,26]		
Tube	ρ (Å^{-2})	e_b (K)
(8,8)	0.0540	-359.4 ± 0.1
(12,12)	0.0612	-371.6 ± 0.1
(16,16)	0.0656	-369.9 ± 0.1
31/75 (δ phase in H_2 on graphite[26])		
Tube	ρ	e_b
(5,5)	0.0421	-334.8 ± 0.1
(10,10)	0.0549	-367.0 ± 0.1

face. The stability limits for the two solids in the (6,6) tube are 0.0755 ± 0.0001 Å^{-2} (e_b = -338.2 ± 0.1 K) and 0.0855 ± 0.0001 Å^{-2} (e_b = -354.1 ± 0.1 K), also obtained by a Maxwell construction. The $1\times\sqrt{3}$ structure defined in Ref. 24 for (n,0) nanotubes was found also to be unstable for all the tubes considered. For instance, for the (16,16) tube, the density of this phase is 0.0750 Å^{-2}, with a binding energy of -303.9 ± 0.6 K.

IV. CONCLUDING REMARKS

Summarizing, we studied all the possible H_2 phases adsorbed on the surface of armchair carbon nanotubes ranging from (5,5) to (16,16). In all cases, but the last one, we have found that the stable phases are incommensurate solids formed by molecules adsorbed on circumferences perpendicular to the main tube axis. Where the curvature of the surface is more relevant, i.e., in the narrowest tubes [(5,5),(6,6)], our results show the existence of a solid-solid zero-temperature phase transition between two incommensurate structures. The first commensurate solid phase, curved version of the well-known $\sqrt{3}\times\sqrt{3}$ phase, appears only when the radius of the nanotube is big enough: a (16,16) tube for H_2.

ACKNOWLEDGMENTS

We acknowledge partial financial support from the Junta de Andalucía group PAI-205 and grant FQM-5985, DGI (Spain) Grants No. FIS2010-18356 and FIS2008-04403, and Generalitat de Catalunya Grant No. 2009SGR-1003.

[1] S. Iijima, Nature (London) **354**, 56 (1991).
[2] K.S. Novoselov, A.K. Geim, S.V. Morozov, D. Jiang, Y. Zhang, S.V. Dubonos, I.V. Grigorieva and A.A. Firsov. Science **306** 666 (2004).
[3] K.S. Novoselov, D. Jiang, F. Schedin, T.J. Booth, V.V. Khotkevich, S.V. Morozov and A.K. Geim. PNAS, **102** 10451 (2005).
[4] S. Talapatra, A.Z. Zambano, S.E. Weber and A.D. Migone, Phys. Rev. Lett. **85** 138 (2000).
[5] M.C. Gordillo. Phys. Rev. Lett. **96** 216102 (2006).
[6] M.C. Gordillo Phys. Rev. B **76** 115402 (2007).
[7] J.V. Pearce, M.A. Adams, O.E. Vilches, M.R. Johnson and H.R. Glyde, Phys. Rev. Lett. **95** 185302 (2005).
[8] M.C. Gordillo. Phys. Rev. Lett. **101** 046102 (2008).
[9] D.S. Greywall, Phys. Rev. B **47** 309 (1993)
[10] M.C. Gordillo and J. Boronat, Phys. Rev. Lett. **102**, 085303 (2009).
[11] H. Freimuth and H. Wiechert, Surf. Sci. **162**, 432 (1985).
[12] H. Wiechert, Physica B **169**, 144 (1991).
[13] M.C. Gordillo and J. Boronat, Phys. Rev. B **81**, 155435 (2010).
[14] T. Wilson, A. Tyburski, M.R. DePies, O.E. Vilches, D. Becquet and M. Bienfait. J. Low Temp. Phys. **126** 403 (2002).
[15] S. Ramachandran, T.A. Wilson, D. Vandervelde, D.K. Holmes and O.E. Vilches. J. Low Temp. Phys. **134** 115 (2004).
[16] S. Talapatra, V. Krungleviciute and A.D. Migone. Phys. Rev. Lett. **89** 246106 (2002).
[17] S. Ramachandran and O.E. Vilches. Phys. Rev. B. **76** 075404 (2007).
[18] C. Tiby, H. Wiechert and H.J. Lauter, Surf. Sci. **119**, 21 (1982)

[19] L.W. Bruch, M.W. Cole, and E. Zaremba, *Physical adsorption: forces and phenomena*, Oxford University Press, Oxford (1997).
[20] Z. Wang, J. Wei, P. Morse, J. G. Dash, O.E. Vilches and D.H. Cobden. Science **327** 552 (2010).
[21] J. Boronat and J. Casulleras, Phys. Rev. B **49**, 8920 (1994).
[22] I. F. Silvera and V. V. Goldman, J. Chem. Phys. **69**, 4209 (1978).
[23] G. Stan and M.W. Cole, J. Low Temp. Phys. **110**, 539 (1998).
[24] A.D. Lueking and M.W. Cole. Phys. Rev. B **75** 195425 (2007).
[25] P. Corboz, M. Boninsegni, L. Pollet and M. Troyer. Phys. Rev. B **78** 245414 (2008).
[26] H. Freimuth, H. Wiechert, H.P. Schildberg and H.J. Lauter. Phys. Rev. B **42** 587 (1990).